MATERIALE PLASTICE
https://revmaterialeplastice.ro
https://doi.org/10.37358/Mat.Plast.1964

The Effect of Mold Conditions on Heat Resistance of Injection-Molded Stereocomplex Polylactide-*b*-polyethylene Glycol-*b*-Polylactide Bioplastic

YODTHONG BAIMARK[1]*, WUTTIPONG RUNGSEESANTIVANON[2], NATCHA PRAKYMORAMAS[2]

[1]Biodegradable Polymers Research Unit, Department of Chemistry and Center of Excellence for Innovation in Chemistry, Faculty of Science, Mahasarakham University, Mahasarakham 44150, Thailand

[2]National Metal and Materials Technology Center (MTEC), 114 Thailand Science Park (TSP), Phahonyothin Road, Khlong Nueng, Khlong Luang, Pathum Thani 12120, Thailand

Abstract: *The effect of mold conditions was investigated in terms of mold temperature (30°C and 90°C) and cooling time (30 s and 60 s) on the heat resistance of injection-molded bars for stereocomplex polylactide-b-polyethylene glycol-b-polylactide (scPLA-PEG-PLA). Comparative study was performed for poly(L-lactide) (PLLA) and PLLA-b-PEG-b-PLLA (PLLA-PEG-PLLA). scPLA-PEG-PLA was 90/10 (w/w) PLLA-PEG-PLLA/poly(D-lactide) blend. scPLA-PEG-PLA exhibited the easiest crystallization upon cooling scan as shown by differential scanning calorimetry (DSC). Higher mold-temperature and longer cooling-time induced higher degree of crystallinity as assessed by X-ray diffractometry (XRD) except for PLLA bars. The heat resistance of both PLLA-PEG-PLLA and scPLA-PEG-PLA bars was improved with increased mold-temperature and cooling-time as shown by dynamic mechanical analysis (DMA), vicat softening temperature (VST) and heat distortion-resistance tests except for PLLA bars. In conclusion, the heat resistance of injection-molded bars prepared at 90˚C mold temperature was in the order scPLA-PEG-PLA > PLLA-PEG-PLLA > PLLA. The results suggested that flexible PLLA-PEG-PLLA and scPLA-PEG-PLA with high degrees of crystallinity were successfully obtained by injection molding for use as good heat-resistant bioplastic products.*

Keywords: *poly(lactic acid), polyethylene glycol, block copolymer, stereocomplex, heat resistance*

1. Introduction

Poly(L-lactic acid) or poly(L-lactide) (PLLA) is an important bio-based plastic because it features non-toxicity, biodegradability, bio-renewability and good processability [1–3]. PLLA and modified PLLA have been successfully utilized in several industrial applications such as biomedical, pharmaceutical, automotive interiors and packaging [2,4–6]. However, low flexibility, poor crystallizability and low heat-resistance were the problems in practical use of PLLA [7–9].

Poly(L-lactide)-*b*-polyethylene glycol-*b*-poly(L-lactide) triblock copolymers (PLLA-PEG-PLLA) showed greater flexibility and faster crystallization-rate than PLLA due to flexibility of PEG middle-blocks causing an enhanced plasticizing effect [10,11]. However, the heat resistance of PLLA-PEG-PLLA was still poor [12]. The heat resistance of PLLA and PLLA-PEG-PLLA is directly related to degree of crystallinity [13–15]. This indicates that crystallizability of PLLA-PEG-PLLA is not enough to improve its heat resistance. Nucleating agents and heat treatment have been used to increase the degree of crystallinity of PLLA and so improve its heat-resistance [13–15].

Poly(D-lactide) (PDLA) has been blended with PLLA to form a stereocomplex polylactides (scPLA) which consisted of homo- and stereocomplex (sc) crystallites [16–19]. The homo- and sc-crystallites of PLA had melting temperatures at lower and higher than 200°C, respectively [20]. The scPLA showed better thermo-mechanical properties and heat resistance than PLLA due to faster crystallization of sc-crystallites upon cooling [19,21,22]. However, scPLA with high PDLA contents or high content of sc-crystallites have to be processed at high temperature (240 – 250°C) which risks thermal decomposition

**email: yodthong.b@msu.ac.th*

[12, 23–25]. Meanwhile PLLA has been blended with small amounts of PDLA for enhancing PLLA crystallization [19, 26–28]. The result was that sc-crystallites can act as nucleating sites to enhance crystallizability of PLLA phases. This process can be performed at 200ºC or below [19,27].

Higher mold-temperature was reported to enhance crystallizability and heat resistance of injection-molded bars for both PLLA [14] and scPLA [29]. However, no reports were present to study optimum mold-conditions for injection-molded bars of flexible PLLA-PEG-PLLA and scPLA-PEG-PLA for these purposes.

This paper studied the effects of mold temperature and cooling time on crystallizability and heat resistance of injection-molded bars of PLLA-PEG-PLLA and scPLA-PEG-PLA. PDLA of 10 wt% was blended with PLLA-PEG-PLLA to form scPLA-PEG-PLA. Annealing effect by post heat-treatment of injection-molded bars was also investigated for comparison. The thermal properties, crystalline structures, mechanical properties and heat resistance of injection-molded bars obtained were determined and discussed. Injection-molded PLLA bars were also prepared and studied for comparison.

2. Materials and methods

2.1. Materials

PLLA grade 3052D was supplied by NatureWork LLC. It had melt flow index (MFI) of 14 g/10 min (210ºC, 2.16 kg). *In situ* chain-extended PLLA-PEG-PLLA with MFI of 26 g/10 min (190ºC, 2.16 kg) was synthesized by ring-opening polymerization of L-lactide monomer in the presence of 2.0 phr Joncryl® ADR4368 (chain extender) according to our previous work [30]. PDLA with number-average molecular weight and dispersity index of 90,000 g/mol and 2.8 from GPC respectively, was synthesized as described in our previous work [25].

2.2. Preparation of injection-molded bars

scPLA-PEG-PLA was prepared by melt blending of 90/10 (w/w) PLLA-PEG-PLLA/PDLA mixture. The mixture was dried overnight at 50ºC in a vacuum oven before melt blending using an internal batch mixer (Hakke Polylab OS system) at 190ºC with a rotor speed of 100 rpm for 4 min. The injection-molded bars with dumbbell (ASTM D 638) and rectangular (ASTM D 790) shapes of PLLA3052D, PLLA-PEG-PLLA and scPLA-PEG-PLA were obtained by injection molding the samples in an injection-molding machine (Nissei Plastic Industrial Co., Ltd., Japan, Model PS40E5ASE) at 170ºC. Mold temperatures and cooling times of 30ºC for 60 s, 90ºC for 30 s and 90ºC for 60 s were used. The obtained bars prepared with mold temperature at 30ºC for 60 s were annealed at 90ºC for 24 h in an air oven in order to study the annealing effect.

2.3. Characterization

Thermal transition properties of PLLA3052D, PLLA-PEG-PLLA and scPLA-PEG-PLA pellets were determined using a Differential Scanning Calorimeter (DSC, Perkin-Elmer, Model Pyris Diamond) under nitrogen gas flow. For DSC heating scan, the sample (3-5 mg) in a sealed aluminum pan was firstly melted at 200ºC for 3 min. to remove thermal history, after which it was quenched to 0ºC before scanning from 0ºC to 200ºC with a heating rate of 10ºC/min. The degree of crystallinity from DSC of the PLA homo-crystallites (DSC-$X_{c,hc}$) was calculated from the enthalpies of melting (ΔH_m) and cold crystallization (ΔH_{cc}) with the following equation.

$$\text{DSC-}X_c\ (\%) = [(\Delta H_m - \Delta H_{cc})/(93.7 \times W_{PLLA})] \times 100 \quad (1)$$

where the values 93.7 J/g is the ΔH_m for 100%X_c PLLA [31]. W_{PLLA} is the PLLA weight-fraction of the samples that is calculated from the PLLA fraction (PLLA =1.00 and PLLA-PEG-PLLA = 0.83 obtained from ^{1}H-NMR) [11].

For DSC cooling scans, the sample was firstly melted at 200°C for 3 min to erase the thermal history before scanning from 200°C to 0°C at a cooling rate of 10°C/min under nitrogen gas flow.

The crystalline structures of injection-molded bars were investigated using a X-Ray Diffractometer (XRD, Bruker, Model D8 Advance) with CuKα radiation at 40 kV and 40 mA. The samples were scanned in the range of 2θ from 5° to 30° at a rate of 3°/min. The degree of crystallinity from XRD for PLA hc-crystallites (XRD-$X_{c,hc}$) and degree of crystallinity from XRD for PLA sc-crystallites (XRD-$X_{c,sc}$) were determined from equations (2) and (3), respectively [32]. Total degree of crystallinity from XRD (XRD-X_c) and percentage of sterecomplex (%SC) were calculated from equations (4) and (5), respectively.

$$\text{XRD-}X_{c,hc}\ (\%) = S_{hc}/(S_{hc} + S_{sc} + S_a) \times 100 \quad (2)$$

$$\text{XRD-}X_{c,sc}\ (\%) = S_{sc}/(S_{hc} + S_{sc} + S_a) \times 100 \quad (3)$$

$$\text{XRD-}X_c\ (\%) = \text{XRD-}X_{c,hc} + \text{XRD-}X_{c,sc} \quad (4)$$

$$\text{SC}\ (\%) = (\text{XRD-}X_{c,sc}/\text{XRD-}X_c) \times 100 \quad (5)$$

where S_{hc}, S_{sc} and S_a are the XRD reflex areas of PLA hc-crystallites and PLA sc-crystallites and of the XRD reflex area of the amorphous halo, respectively.

Tensile properties of injection-molded bars were investigated using a Universal Testing Machine (Instron Model 4052) at 25°C according to ASTM D 638 type I with a cross-head speed of 5 mm/min. At least five bars of each sample were tested to calculate the average value.

Thermo-mechanical properties of injection-molded bars, 3 × 13 × 60 mm in size, were tested using a Dynamic Mechanical Analyzer (DMA, TA Instruments Model Q800) in a multi-frequency strain mode. The samples were heated at a rate of 2°C/min from 30°C to 140°C at a scan amplitude of 20 μm and a scan frequency of 1 Hz.

The heat deflection temperature (HDT) of injection-molded bar samples was measured using a HDT/Vicat machine (Yasuda, Model HD-PC). The bar samples were 3 × 13 × 125 mm in size and were heated in silicone oil at a rate of 2°C/min under 0.455 MPa load according to ASTM D 648-01. The HDT value was obtained for a 0.25 mm deflection of the bar sample. Average value was obtained from triplicate measurements.

The Vicat softening temperature (VST) of injection-molded bar samples was determined using a HDT/Vicat machine (Yasuda, Model HD-PC). Bar samples (3 × 20 × 20 mm) were heated in silicone oil at a rate of 2°C/min under 50 N load of a flat-ended needle according to ISO 306. A surface area of a flat-ended needle was 1 mm^2. The VST value was obtained when the needle penetrated the sample by 1 mm. Average value was obtained from triplicate measurements.

Heat distortion resistance of injection-molded bars was directly observed by half hanging in an oven at 85°C for 5 min by following the method [9] with some modifications. Photographs of bar samples after the test were recorded to compare heat deformation of bar samples.

3. Results and discussion

3.1. Thermal transition properties

DSC method was used to determine the thermal transition properties of samples including glass transition temperature (T_g), cold-crystallization temperature (T_{cc}), enthalpy of cold crystallization (ΔH_{cc}), melting temperature (T_m) and enthalpy of melting (ΔH_m) from DSC heating curves (Figure 1(above)) as well as crystallization temperature (T_c) and enthalpy of crystallization (ΔH_c) from DSC cooling curves (Figure 1(below)). The DSC results are summarized in Table 1.

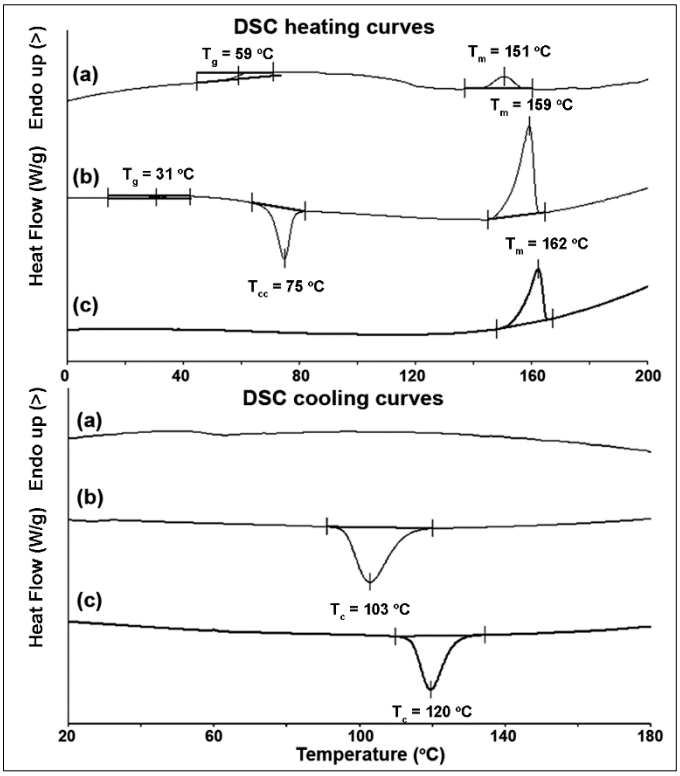

Figure 1. DSC heating curves (above) and cooling curves (below) of (a) PLLA3052D, (b) PLLA-PEG-PLLA and (c) scPLA-PEG-PLA

Table 1. DSC results of samples.

Samples	T_g (˚C)[a]	T_{cc} (˚C)[a]	ΔH_{cc} (J/g)[a]	T_m (˚C)[a]	ΔH_m (J/g)[a]	DSC-$X_{c,hc}$ (%)[a]	T_c (˚C)[b]	ΔH_c (J/g)[b]
PLLA3052D	59	-	-	151	6.2	6.6	-	-
PLLA-PEG-PLLA	31	75	16.3	159	33.4	22.0	103	29.5
scPLA-PEG-PLA	-	-	-	162	19.4	24.4	120	20.6

[a] Obtained from DSC heating scan.
[b] Obtained from DSC cooling scan.

From DSC heating curves, T_g of PLLA3052D was 59ºC while PLLA-PEG-PLLA exhibited a lower T_g at 31ºC. This seemed to due to plasticizing effect of flexible PEG middle-blocks [10,11]. T_g of scPLA-PEG-PLA could not be detected. From DSC cooling curves, PLLA3052D had no T_c peak. PLLA-PEG-PLLA and scPLA-PEG-PLA had a T_c at 103ºC and 120ºC, respectively indicating that crystallization upon cooling of scPLA-PEG-PLA was easier than that of PLLA-PEG-PLLA. sc-crystallites in scPLA-PEG-PLA enhanced crystallization of PLLA end-blocks by acting as nucleating sites [26-28]. T_m of sc-crystallites in PLLA-PEG-PLLA/PDLA blends were higher than 200ºC. Thus, sc-crystallites did not melt during removal of their thermal history at 200ºC and acted as nucleating sites during the cooling scan [26].

3.2. Crystalline structures

The crystalline structures of injection-molded bars were estimated from XRD patterns as shown in Figure 2. PLLA3052D bars prepared at 30ºC mold temperature for 60 s had no XRD reflexes indicating that they were completely amorphous. The small XRD reflexes of PLLA homo-crystallites (hc) at 2θ = 16.8º [33,34] were found for both PLLA3052D bars prepared at 90ºC mold temperatures for 30 s and 60s. Therefore, increasing the mold temperature from 30ºC to 90ºC had a little effect on crystallization of hc. PLLA3052D bars annealed at 90ºC for 24 h showed four XRD reflexes at 2θ = 14.8º, 16.8º, 19.1º and 22.1º of hc [33,34]. The XRD reflexes of annealed bars had the highest intensity.

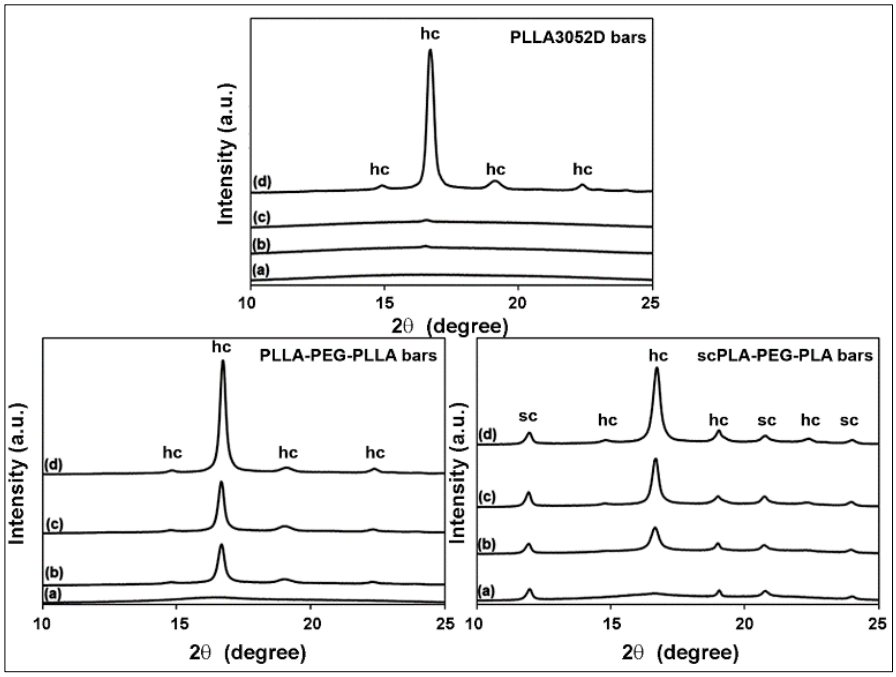

Figure 2. XRD patterns of injection-molded bars for PLLA3052D, PLLA-PEG-PLLA and scPLA-PEG-PLA prepared with mold temperatures and cooling times of (a) 30°C for 60 s, (b) 90°C for 30s and (c) 90°C for 60 s as well as (d) annealed at 90°C for 24 h

The injection-molded bars of PLLA-PEG-PLLA prepared at 30°C mold temperature for 60 s were also completely amorphous. However, XRD reflexes at 2θ = 14.8°, 16.8°, 19.1° and 22.1° for hc were clearly apparent when the mold temperature was increased from 30°C to 90°C for both the cooling times. This indicates that 90°C mold temperature enhanced hc formation of injection-molded PLLA-PEG-PLLA bars.

The injection-molded bars of scPLA-PEG-PLA prepared at 30°C mold temperature for 60 s showed XRD reflexes at 2θ = 16.8° and 19.1° for hc and at 2θ = 11.9°, 20.6° and 23.8° for sc-crystallites [33,35]. When the mold temperature was increased up to 90°C, the XRD reflexes at 2θ = 14.8° and 22.1° of hc appeared for both the cooling times suggesting that higher mold-temperature enhanced PLLA homo-crystallization. The annealed scPLA-PEG-PLA bars exhibited XRD reflexes of both hc and sc-crystallites.

The degrees of crystallinity of injection-molded bars from XRD are summarized in Table 2. It can be seen that at 90°C mold temperature for both the cooling times could not significantly improve crystallization of injection-molded PLLA3052D bars. The XRD-$X_{c,hc}$ of PLLA3502D bars was increased up to 51.7% when they were annealed at 90°C for 24 h. The XRD-$X_{c,hc}$ of PLLA-PEG-PLLA bars prepared at 90°C mold temperature were higher than PLLA3052D. The flexible PEG middle-blocks enhanced chain mobility to improve PLLA end-block crystallization of PLLA-PEG-PLLA by a plasticizing effect [10]. The XRD-$X_{c,hc}$ of PLLA-PEG-PLLA bars prepared at 90°C mold temperature increased from 25.6% to 30.8% as the cooling time was increased. The annealed PLLA-PEG-PLLA bars exhibited the highest XRD-$X_{c,hc}$ (46.2%).

The scPLA-PEG-PLA bars prepared at 30°C mold temperature had the XRD-$X_{c,hc}$ and XRD-$X_{c,sc}$ of 1.4% and 11.2%, respectively. Both the XRD-$X_{c,hc}$ and XRD-$X_{c,sc}$ of scPLA-PEG-PLA bars prepared at 90°C mold temperature steadily increased as the cooling time increased from 30 to 60 s. The XRD-X_c of scPLA-PEG-PLA bars increased and %SC decreased with the increase of mold temperature and cooling time. The annealed scPLA-PEG-PLA bars had the highest XRD-X_c (53.1%) and the lowest %SC (26.0%). It should be noted that the XRD-X_c of scPLA-PEG-PLA bars were larger than those of PLLA-PEG-PLLA bars at the same mold temperature and cooling time. This suggests higher crystallizability of the scPLA-PEG-PLA bars. The crystallinity of injection-molded PLLA bars cannot be largely improved at mold temperature less than 100°C [15]. But the injection-molded bars of PLLA-PEG-PLLA and scPLA-PEG-PLA exhibited largely increased in their crystallinity contents at 90°C mold temperature.

Table 2. Degrees of crystallinity from XRD of injection-molded bars.

Injection-molded bars	XRD-$X_{c,hc}$ (%)	XRD-$X_{c,sc}$ (%)	XRD-X_c (%)	SC (%)
PLLA3052D				
30˚C for 60 s	-	-	-	-
90˚C for 30 s	0.3	-	0.3	-
90˚C for 60 s	0.4	-	0.4	-
annealed at 90 ˚C for 24 h	51.7	-	51.7	-
PLLA-PEG-PLLA				
30˚C for 60 s	-	-	-	-
90˚C for 30 s	25.6	-	25.6	-
90˚C for 60 s	30.8	-	30.8	-
annealed at 90 ˚C for 24 h	46.2	-	46.2	-
scPLA-PEG-PLA				
30˚C for 60 s	1.4	11.2	11.2	88.9
90˚C for 30 s	15.8	11.8	27.6	42.8
90˚C for 60 s	27.6	16.7	44.3	37.7
annealed at 90 ˚C for 24 h	39.3	13.8	53.1	26.0

3.3. Mechanical properties

The mechanical properties of injection-molded bars were determined by tensile tests as summarized in Table 3. The ultimate tensile stress of PLLA3052D bars prepared with different mold-conditions and annealing were in range 57.1–63.2 MPa suggesting that the XRD-X_c changes of PLLA3052D bars did not significantly affect the ultimate tensile stress. However, the strain at break slightly decreased and Young's modulus increased as the mold temperature and cooling time increased. This may be explained by an increasing XRD-X_c of PLLA3052D bars inhibiting chain mobility for extension of bar samples and improving their stiffness [14].

With increasing mold temperature and cooling time, the ultimate tensile stress and Young's modulus of PLLA-PEG-PLLA and scPLA-PEG-PLA bars increased as well as strain at break decreased. It should be noted that their strains at break dramatically dropped as the mold temperature was increased. This is due to the XRD-X_c largely increasing as the mold temperature increased (Table 2). All the annealed bars with the high XRD-X_c exhibited the highest tensile stress and Young's modulus whereas they had the lowest strain at break. However, both the PLLA-PEG-PLLA and scPLA-PEG-PLA bars exhibited strain at break higher than the PLLA3052D indicated they were more flexible than the PLLA3052D. Finally, the tensile properties of the scPLA-PEG-PLA bars were better than the PLLA-PEG-PLLA bars. This can be explained by the sc-crystallites enhanced mechanical properties by acting as physical cross-linking sites in amorphous regions [36].

Table 3. Tensile properties, HDT and VST of injection-molded bars

Injection-molded bars	Ultimate tensile stress, (MPa)	Strain at break, (%)	Young's modulus (MPa)	HDT (˚C)	VST (˚C)
PLLA3052D					
30 ˚C for 60 s	60.6 ± 0.7	4.7 ± 0.8	3,708 ± 56	45.9 ± 0.2	56.5 ± 0.3
90 ˚C for 30 s	57.8 ± 1.1	3.0 ± 0.4	4,040 ± 268	46.9 ± 0.1	57.0 ± 0.4
90 ˚C for 60 s	57.1 ± 1.8	2.6 ± 0.5	4,383 ± 127	46.6 ± 0.2	57.0 ± 0.2
annealed at 90 ˚C for 24 h	63.2 ± 3.9	2.0 ± 0.2	5,157 ± 684	63.2 ± 0.6	83.4 ± 2.4
PLLA-PEG-PLLA					
30 ˚C for 60 s	19.1 ± 0.9	101.8 ± 8.1	1,038 ± 40	38.9 ± 0.4	42.6 ± 0.1
90 ˚C for 30 s	18.9 ± 1.7	6.2 ± 1.9	1,019 ± 64	43.0 ± 3.2	60.6 ± 5.9
90 ˚C for 60 s	20.3 ± 0.8	6.8 ± 0.2	1,163 ± 128	45.9 ± 3.5	60.5 ± 0.3
annealed at 90 ˚C for 24 h	21.7 ± 2.9	5.4 ± 0.5	1,208 ± 72	53.9 ± 2.2	70.0 ± 2.1
scPLA-PEG-PLA					
30 ˚C for 60 s	22.6 ± 0.6	151.3 ± 22.8	1,479 ± 136	41.8 ± 0.5	48.3 ± 1.1
90 ˚C for 30 s	24.6 ± 0.3	31.4 ± 2.73	1,592 ± 18	43.4 ± 2.3	64.2 ± 0.6
90 ˚C for 60 s	24.8 ± 0.6	18.4 ± 1.8	1,634 ± 289	49.9 ± 0.6	65.2 ± 0.4
annealed at 90 ˚C for 24 h	28.7 ± 0.8	7.8 ± 2.2	1,664 ± 143	57.1 ± 1.5	74.5 ± 0.4

3.4. DMA

The DMA method has been widely used to investigate heat resistance of PLLA and modified PLLA using storage-modulus change as a function of temperature [16,19,22,37,38]. Usually, the storage modulus of PLLA is high at temperature below its T_g (around 60°C) because it is in the glassy state. The storage modulus of PLLA drastically dropped when the temperature passed the T_g region before increasing again caused by cold crystallization of PLLA [16]. This demonstrates the PLLA has poor heat-resistance due to its low degree of crystallinity after melt processing.

Figure 3 shows the storage-modulus changes on temperature of injection-molded bars. From Figure 3a, all the PLLA3052D bars prepared with mold temperatures at 30°C and 90°C exhibited large decreases of the storage moduli in the T_g region (60–80°C) suggesting that they had poor heat-resistance. This could be explained by the PLLA3052D bars containing low XRD-X_c. Whereas the annealed PLLA3052D bars were slightly decreased in storage modulus indicated that they were good heat-resistance. This is because the PLLA3052D bars had the highest XRD-X_c. The results confirmed that the PLLA with high X_c exhibited good heat-resistance [14,16,19].

For PLLA-PEG-PLLA and scPLA-PEG-PLA bars, the lowest storage-moduli increased with the mold temperature and cooling time as shown in Figures 3b and 3c, respectively. The results suggested that the heat resistance of both PLLA-PEG-PLLA and scPLA-PEG-PLA bars were improved by increasing the mold temperature and cooling time. The annealed PLLA-PEG-PLLA and scPLA-PEG-PLA bars showed the best heat-resistance. This is due to higher mold-temperature and longer cooling-time of injection-molded bars induced greater XRD-X_c.

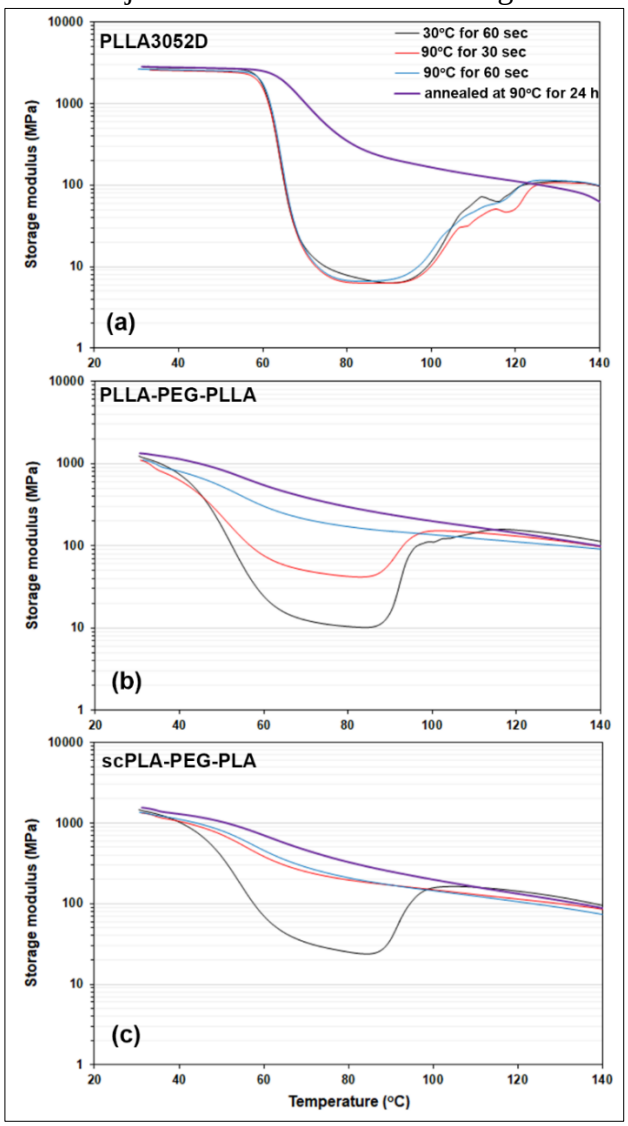

Figure 3. DMA curves of injection-molded bars of (a) PLLA3052D, (b) PLLA-PEG-PLLA and (c) scPLA-PEG-PLA

The storage moduli at 85ºC of injection-molded bars were compared in Figure 4. A temperature at 85ºC was selected for comparison because the storage moduli increased again after 85ºC due to cold-crystallization effects. All the injection-molded bars prepared at 30ºC mold temperature had low storage moduli (Figure 4a). The storage moduli at 85ºC increased significantly as the mold temperature increased from 30 to 90ºC and cooling time increased from 30 to 60 s except PLLA3052D bars (Figure 4b and 4c). All the annealed bars showed the highest storage moduli at 85ºC (Figure 4d). From DMA results, it can be concluded that the heat resistance of injection-molded bars are in order scPLA-PEG-PLA > PLLA-PEG-PLLA > PLLA3052D for the same mold-temperature and cooling-time.

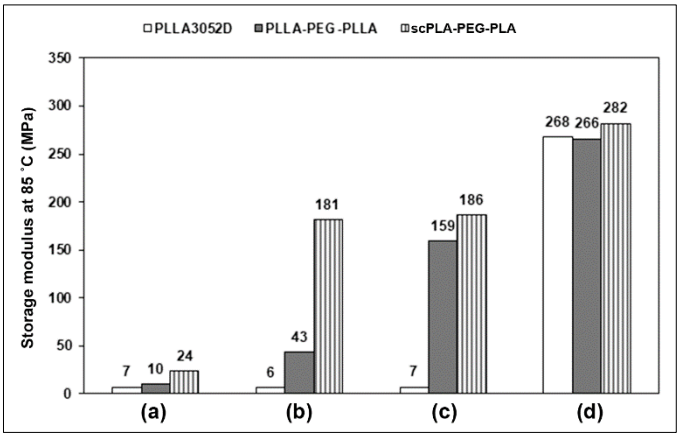

Figure 4. Storage moduli of injection-molded bars prepared with mold temperatures and cooling times of (a) at 30ºC for 60 s, (b) at 90ºC for 30 s and (c) at 90ºC for 60 s as well as (d) annealed at 90ºC for 24 h

3.5. HDT and VST

HDT and VST have been used to determine the heat resistance of injection-molded PLLA bars [9,17]. The resulting HDT and VST are also summarized in Table 3. The HDT and VST of PLLA3052D bars did not significantly change with the mold temperature and cooling time that were in ranges 45.9-46.9ºC and 56.5-57.0ºC, respectively. However, the HDT and VST were increased to 63.2ºC and 83.4ºC, respectively for the annealed PLLA3052D bars.

The HDT of PLLA-PEG-PLLA and scPLA-PEG-PLA bars increased steadily with the mold temperature and cooling time. It can be said that the HDT and VST of these injection-molded bars also depended on their XRD-X_c. The results supported the conclusion that increasing mold-temperatures and cooling-times improved heat resistance of injection-molded bars. It should be noted that the HDT of both PLLA-PEG-PLLA and scPLA-PEG-PLA bars were lower than PLLA3052D bars. This may be due to the fact tha PLLA-PEG-PLLA and scPLA-PEG-PLA are more flexible than PLLA3052D as observed from the results of strain at break from tensile test.

3.6. Heat Distortion Resistance

A half-hanging test was performed in an air oven at 85ºC for 5 min to investigate the heat-distortion resistance of injection-molded bars. The photographs of injection-molded bars after test are shown in Figure 5.

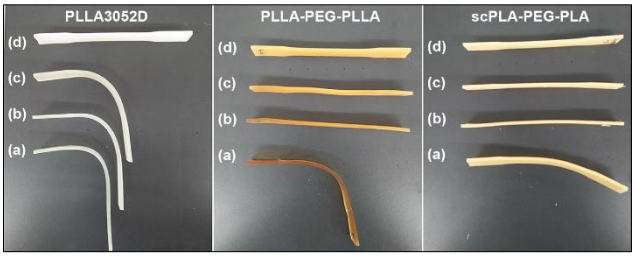

Figure 5. Heat distortion resistance at 85°C for 5 min of injection-molded bars of PLLA3052D, PLLA-PEG-PLLA and scPLA-PEG-PLA prepared with mold temperatures and cooling times of (a) at 30°C for 60 s, (b) at 90°C for 30 s and (c) at 90°C for 60 s as well as (d) annealed at 90°C for 24 h

It can be seen that all the PLLA3052D bars prepared with mold temperatures at 30°C and 90°C were largely deformed indicating that they had poor heat-resistance (Figure 5(left)). Whereas the annealed PLLA3052D bars retained original shape after the test corresponding to the results of DMA, HDT and VST as described above. The annealed PLLA3052D bars had the highest storage-modulus at 85°C (from DMA), HDT and VST.

PLLA-PEG-PLLA and scPLA-PEG-PLA bars were deformed after the test when the mold temperature was at 30°C as shown in Figure 5(middle, a) and 5(right, a), respectively. This is due to their low storage-moduli at 85°C (from DMA), HDT and VST. When the mold temperature was at 90°C, the PLLA-PEG-PLLA and scPLA-PEG-PLA bars exhibited good heat-distortion resistance for both the cooling times because their storage moduli at 85°C (from DMA), HDT and VST increased with the mold temperature. The annealed bars of both PLLA-PEG-PLLA and scPLA-PEG-PLA showed good heat-distortion resistance because their storage moduli at 85°C (from DMA), HDT and VST were the highest. It is worth mentioning that the degree of crystallinity of the injection-molded bars plays the key role in heat-distortion resistance.

It should be noticed that the injection-molded bars with the VST higher than 60°C exhibited good heat-distortion resistance. While the HDT values of the PLLA-PEG-PLLA bars prepared at 90°C mold temperature were lower than the PLLA3052D bars but they showed better heat-distortion resistance than PLLA3052D bars. This is due to the PLLA-PEG-PLLA being softer and more flexible than the PLLA [39,40]. The results indicated that the VST were more reliable than the HDT as heat-resistance parameters as shown in the literature [17]. In addition, the results of DMA and heat-distortion resistance in this work could be used to support the VST results for heat-resistant property of PLLA-based bioplastics.

4. Conclusions

In this work, the effects of mold temperature and cooling time on heat resistance of injection-molded bars were investigated for scPLA-PEG-PLA compared with PLLA3052D and PLLA-PEG-PLLA. DSC results indicated the crystallizability of samples was in order scPLA-PEG-PLA > PLLA-PEG-PLLA > PLLA3052D. From XRD, both the PLLA3052D and PLLA-PEG-PLLA bars prepared at 30°C mold temperature were completely amorphous in character whereas the scPLA-PEG-PLA bars had both hc and sc-crytsallites. The XRD-X_c of PLLA-PEG-PLLA and scPLA-PEG-PLA bars increased with the mold temperature and cooling time but PLLA3052D bars did not. Increasing the mold temperature and cooling time improved the heat resistance of injection-molded bars for both PLLA-PEG-PLLA and scPLA-PEG-PLA except for PLLA3052D bars as observed from their increasing the lowest storage-moduli from the DMA study, HDT, VST and heat-distortion resistance.

It can be concluded that the 90°C mold temperature seem to improve the XRD-X_c and heat resistance of both the injection-molded bars for PLLA-PEG-PLLA and scPLA-PEG-PLA except for PLLA3052D.

The results could provide guidance toward fabrication of high heat-resistant and flexible scPLA-PEG-PLA at industrial scale for use as bioplastic products.

Acknowledgements. This research was funded by The National Research Council of Thailand (NRCT) and the Biodiversity-based Economy Development Office (BEDO). The Center of Excellence for Innovation in Chemistry (PERCH-CIC), Office of the Higher Education Commission, Ministry of Education, Thailand is also acknowledged.

References

1. ROCCA-SMITH, J.R., WHYTE, O., Brachais C.H., CHAMPION, D., PIASENTE, F., MARCUZZO, E., SENSIDONI, A., DEBEAUFORT, F., KARBOWIAK, T., Beyond biodegradability of poly(lactic acid): physical and chemical stability in humid environments, *ACS Sustainable Chem. Eng.*, **5**, 2017, 2751−2762.
2. SILVA, D., KADURI, M., POLEY, M., ADIR, O., KRINSKY, N., SHAINSKY-ROTIMAN, J., SCHROEDER, A., Biocompatibility, biodegradation and excretion of polylactic acid (PLA) in medical implants and theranostic systems, *Chem. Eng. J.*, **340**, 2018, 9−14.
3. CASTRO-AGUIRRE, E., AURAS, R., SELKE, S., RUBINO, M., MARSH, T., Enhancing the biodegradation rate of poly(lactic acid) films and PLA bio-nanocomposites in simulated composting through bioaugmentation, *Polym. Degrad. Stab.*, **154**, 2018, 46−54.
4. SADEGHI-AVALSHAHR, A., KHORSAND-GHAYENI, M., NOKHASTEH, S., SHAHRI, M.M., MOLAVI, A.M., SADEGHI-AVALSHAHR, M., Effects of hydroxyapatite (HA) particles on the PLLA polymeric matrix for fabrication of absorbable interference screws, *Polym. Bull.*, **75**, 2018, 2559−2574.
5. LOGANATHAN, S., JACOB, J., VALAPA, R.B., THOMAS, S., Influence of linear and branched amine functionalization in mesoporous silica on the thermal, mechanical and barrier properties of sustainable poly(lactic acid), *Polymer*, **148**, 2018, 149−157.
6. HONGTHIPWAREE, T., SRIAMORNSAK, P., SEADAN, M., SUTTIRUENGWONG, S., Effect of cosolvent on properties of non-woven porous neomycin-loaded poly(lactic acid)/polycaprolactone fibers, *Mater. Today Sustainability*, **10**, 2020, 100051.
7. GAO, C., GUO, J., XIE, H., The effect of alginate on the mechanical, thermal, and rheological properties of nano calcium carbonate-filled polylactic acid composites, *Polym. Eng. Sci.*, **59**, 2019, 1882−1888.
8. HUANG, H., ZHANG, Y.H., ZHAO, L.S., LUO, G.M., CAI, Y.H., Insight into the role of a isophthalic dihydrazide derivative containing piperonylic acid in poly(L-lactide) nucleation: thermal performances and mechanical properties, *Mater. Plast.*, **57**(3), 2020, 28−40.
9. GAO, X.R., NIU, B., HUA, W.Q., LI, Y., XU, L., WANG, Y., JI, X., ZHONG, G.J., LI, Z.M., Rapid preparation and continuous processing of polylactide stereocomplex crystallite below its melting point, *Polym. Bull.*, **76**, 2019, 3371−3385.
10. YUN, X., LI, X., JIN, Y., SUN, W., DONG, T., Fast crystallization and toughening of poly(L-lactic acid) by incorporating with poly(ethylene glycol) as a middle block chain, *Polym. Sci. Series A*, **60**, 2018, 141−155.
11. BAIMARK, Y., RUNGSEESANTIVANON, W., PRAKYMORAMAS, N., Improvement in melt flow property and flexibility of poly(L-lactide)-*b*-poly(ethylene glycol)-*b*-poly(L-lactide) by chain extension reaction for potential use as flexible bioplastics, *Mater. Des.*, **154**, 2018, 73−80.
12. PASEE, S., BAIMARK, Y., Improvement in mechanical properties and heat resistance of PLLA-*b*-PEG-*b*-PLLA by melt blending with PDLA-*b*-PEG-*b*-PDLA for potential use as high-performance bioplastics, *Adv. Polym. Technol.*, **2019**, 2019, Article ID 8690650.
13. LI, H., HUNEAULT, M.A., Effect of nucleation and plasticization on the crystallization of poly(lactic acid), *Polymer*, **48**, 2007, 6855−6866.

14. VADORI, R., MOHANTY, A.K., MISRA, M., The effect of mold temperature on the performance of injection molded poly(lactic acid)-based bioplastic, *Macromol. Mater. Eng.*, **298**, 2013, 981–990.
15. ZHANG, X., MENG, L., LI, G., LIANG, N., ZHANG, J., ZHU, Z., WANG, R., Effect of nucleating agents on the crystallization behavior and heat resistance of poly(L-lactide), *J. Appl. Polym. Sci.*, **133**, 2016, 42999.
16. PAN, H., KONG, J., CHEN, Y., ZHANG, H., DONG, L., Improved heat resistance properties of poly(L-lactide)/basalt fiber biocomposites with high crystallinity under forming hybrid-crystalline morphology, *Int. J. Biol. Macromol.*, **122**, 2019, 848–856.
17. PEELMAN, N., RAGAERT, P., RAGAERT, K., ERKOC, M., BREMPT, W.V., FAELENS, F., DEVLIEGHERE, F., MEULENAER, B.D., CARDON, L., Heat resistance of biobased materials, evaluation and effect of processing techniques and additives, *Polym. Eng. Sci.*, **58**, 2018, 513–520.
18. PAN, G., XU, H., MU, B., YANG, J., YANG, Y., Complete stereo-complexation of enantiomeric polylactides for scalable continuous production, *Chem. Eng. J.*, **328**, 2017, 759–767.
19. SI, W.J., AN, X.P., ZENG, J.B., CHEN, Y.K., WANG, Y.Z., Fully bio-based, highly toughened and heat-resistant poly(L-lactide) ternary blends via dynamic vulcanization with poly(D-lactide) and unsaturated bioelastomer, *Sci. China Mater.*, **60**, 2017, 1008–1022.
20. PHATTARATEERA, S., PATTAMAPROM, C., The effect of different acrylic-based rubbers on the crystallization behavior of PLA/PDLA stereocomplex, *J. Polym. Environ.*, **28**, 2020, 1592–1600.
21. ANDERSON, K.S., HILLMYER, M.A., Melt preparation and nucleation efficiency of polylactide stereocomplex crystallites, *Polymer*, **47**, 2006, 2030–2035.
22. KUROKAWA, N., HOTTA, A., Thermomechanical properties of highly transparent self-reinforced polylactide composites with electrospun stereocomplex polylactide nanofibers, *Polymer*, **153**, 2018, 214–222.
23. XU, H., TANG, S., CHEN, J., YIN, P., PU, W., LU, Y., Thermal and phase-separation behavior of injection-molded poly(L-lactic acid)/poly(D-lactic acid) blends with moderate optical purity, *Polym. Bull.*, **68**, 2012, 1135–1151.
24. EL-KHODARY, E., FUKURI, Y., YAMAMOTO, M., YAMANE, H., Effect of the melt-mixing condition on the physical property of poly(L-lactic acid)/poly(D-lactic acid) blends, J. *Appl. Polym. Sci.*, **134**, 2017, 45489.
25. BAIMARK, Y., KITTIPOOM, S., Influence of chain-extension reaction on stereocomplexation, mechanical properties and heat resistance of compressed stereocomplex-polylactide bioplastic films, *Polymers*, **10**, 2018, 1218.
26. YAMANE, H., SASAI, K., Effect of the addition of poly(D-lactic acid) on the thermal property of poly(L-lactic acid), *Polymer*, **44**, 2003, 2569–2575.
27. WEI, X.F., BAO, R.Y., CAO, Z.Q., YANG, W., XIE, B.H., YANG, M.B., Stereocomplex crystallite network in asymmetric PLLA/PDLA blends: formation, structure, and confining effect on the crystallization rate of homocrystallites, *Macromolecules*, **47**, 2014, 1439–1448.
28. ALIOTTA, L., CINELLI, P., COLTELLI, M.B., RIGHETTI, M.C., GAZZANO, M., LAZZERI, A., Effect of nucleating agents on crystallinity and properties of poly(lactic acid) (PLA), *Euro. Polym. J.*, **93**, 2017, 822–832.
29. ZHANG, Z.C., GAO, X.R., HU Z.J., YAN, Z., XU, J.Z., XU, L., ZHONG, G.J., LI, Z.M., Inducing stereocomplex crystals by template effect of residual stereocomplex crystals during thermal annealing of injection-molded polylactide, *Ind. Eng. Chem. Res.*, **55**, 2016, 10896–10905.
30. BAIMARK, Y., RUNGSEESANTIVANON, W., PRAKYMORAMAS, N., Synthesis of flexible poly(L-lactide)-*b*-polyethylene glycol-*b*-poly(L-lactide) bioplastics by ring-opening polymerization in the presence of chain extender, *e-Polymers*, **20**, 2020, 423–429.
31. LI, Z., LIU, L., RAO, Y., RAN, L., WU, T., NIE, R., ANNA, D.S., LI, Y., CHE, Z., Mechanical and antibacterial properties of oriented poly(lactic acid), *Polym. Eng. Sci.*, **59**, 2019, 2121–2127.

32. PHOLHARN, D., SRITHEP, Y., MORRIS, J., Melt compounding and characterization of poly(lactide) stereocomplex/natural rubber composites, *Polym. Eng. Sci.*, **58**, 2018, 713–718.
33. SONG, Y., WANG, D., JIANG, N., GAN, Z., Role of PEG segment in stereocomplex crystallization for PLLA/PDLA-*b*-PEG-*b*-PDLA blends, *ACS Sustainable Chem. Eng.*, **3**, 2015, 1492−1500.
34. JING, Z., SHI, X., ZHANG, G., LEI, R., Investigation of poly(lactide) stereocomplexation between linear poly(L-lactide) and PDLA-PEG-PDLA tri-block copolymer, *Polym. Int.*, **64**, 2015, 1399−1407.
35. JING, Z., SHI, X., ZHANG, G., Competitive stereocomplexation and homocrystallization behaviors in the poly(lactide) blends of PLLA and PDLA-PEG-PDLA with controlled block length, *Polymers*, **9**, 2017, 107.
36. SHI, X., JING, Z., ZHANG, G., Influence of PLA stereocomplex crystals and thermal treatment temperature on the rheology and crystallization behavior of asymmetric poly(L-lactide)/poly(D-lactide) blends, *J. Polym. Res.*, **25**, 2018, 71.
37. NUZZO, A., COIAI, S., CARROCCIO, S.C., DINTCHEVA, N.T., GAMBAROTTI, C., FILIPPONE, G., Heat-resistant fully bio-based nanocomposite blends based on poly(lactic acid), *Macromol. Mater. Eng.*, **299**, 2014, 31–40.
38. MASUTANI, K., KOBAYASHI, K., KIMURA, Y., LEE, C.W., Properties of stereo multi-block polylactides obtained by chain-extension of stereo tri-block polylactides consisting of poly(L-lactide) and poly(D-lactide), *J. Polym. Res.*, **25**, 2018, 74.
39. HAN, L., YU, C., ZHOU, J., SHAN, G., BAO, Y., YUN, X., DONG, T., PAN, P. Enantiomeric blends of high-molecular-weight poly(lactic acid)/poly(ethylene glycol) triblock copolymers: enhanced stereocomplexation and thermomechanical properties, *Polymer*, **103**, 2016, 376–386.
40. BAIMARK, Y, PASEE, S, RUNGSEESANTIVANON, W., PRAKYMORAMAS, N., Influence of chain extension on thermal and mechanical properties of injection-molded poly(L-lactide)-*b*-poly(ethylene glycol)-*b*-poly(L-lactide) bioplastic, *Asian J. Sci. Res.*, **12**, 2019, 508−515.

Manuscript received: 13.12.2020